

ELECTROMAGNETIC WAVE DIRECTION FINDING AS USEFUL TOOL FOR ANALYZING PLANETARY RADIO EMISSIONS: WHICH INFORMATION CAN BE OBTAINED?

H. P. Ladreiter*

Abstract

The attempt of electromagnetic wave direction finding for radio astronomers is the determination of the angle of arrival and the full polarization state of incoming radio emissions from distant sources in the planetary environment. Due to the close distances with respect to such radiation sources during planetary flybys, the technique is useful only for spaceborne antenna systems. Well defined results are obtained when the incident radiation can be regarded as plane waves and when the dimension of the receiving antenna system is much less compared to the wavelengths of interest. Although the reception of the emission is usually performed with monopole or dipole antennas with large antenna pattern, the accuracy of the retrieval of the angular direction of the incoming radiation is in the order of one degree at favorable observation conditions. We outline the mathematical treatment of the problem which leads to this high accuracy based on observations of the Ulysses spacecraft which encountered Jupiter in early 1992 and give expectations for the Cassini spacecraft mission which is dedicated to analyze the environment of Saturn and therefore also the corresponding radio emissions with direction finding capabilities.

1 Introduction

The method of direction finding is a convenient method which serves as monitor for various wave phenomena as planetary radio and plasma waves. In particular, direction finding means the determination of the polarization (characterized by the 4 Stokes parameters, as described by Kraus [1966]) and the direction of incidence of a plane electromagnetic wave based on the analysis of observed signals y_i^{obs} created by the wave on a specific instrument (antenna and receiver system). The form of the observed signals y_i^{obs} depends on the design of the antenna/receiver system in operation. The Unified Radio and Plasma Wave

*Space Research Institute of the Austrian Academy of Sciences, Graz, AUSTRIA

(URAP) experiment on board the Ulysses spacecraft [Stone et al., 1992a] collects the necessary information during one spacecraft spin period (12 seconds) and allows direction finding from the modulation of the signals received with two antennas (one dipole in the spin plane, one monopole along the spin axis) during the spin period. This method tacitly requires the assumption of constant source and wave characteristics during that period. In contrast to Ulysses which is a rotating spacecraft, the Cassini spacecraft is three-axis stabilized and is provided with three linearly independent radio antennas and corresponding receivers. This alternative design enables the Radio and Plasma Wave Science (RPWS) experiment on the Cassini spacecraft to perform direction finding using seven (quasi-) simultaneous measurements providing high time resolution of the derived wave properties.

Interest in direction finding performed by spaceborne instruments as a diagnostic tool for planetary and solar radio emissions increased in the late 70ies. Lecacheux [1978] derived analytical expressions relating the wave polarization and the source direction to measured wave signals for both, a three-axis stabilized spacecraft and antenna configuration and a spinning configuration. Those expressions can, with some modifications, be applied to Ulysses and Cassini direction finding analyses. Manning and Fainberg [1980] developed a methodology for direction finding as performed by the URAP experiment on the Ulysses spacecraft and included the source size as seventh unknown parameter to the analysis (usually, only the wave polarization (described by the four Stokes parameters) and the source direction angles (described by two spherical angles) are introduced). In addition to their approach using a least squares solution by minimizing the sum of the squared differences between observations and model, they suggested a closed form solution as alternative way to derive the wave properties (polarization, source direction and size) directly from the instrument measurements. The least square method has also been used by Reiner et al. [1993a,b] to determine the radiation properties and source location of the Jovian hectometric and narrowband kilometric radio emissions and the closed form solution was adapted by Ladreiter et al. [1994] for positioning the sources and deriving the characteristics of the Jovian hectometric and broadband kilometric radio emissions.

In this paper the methodology of direction finding analysis is presented by using singular value decomposition techniques which present the derived information in a very precise and comprehensive way and allow detailed error propagation analysis. Those so-called generalized inversion techniques allow detailed analysis of the stability of solutions obtained from simultaneously solved systems of equations which result from a least squares formalism.

2 Direction Finding Formalism based on Generalized Inversion

In order to find the model parameter vector X_j that contains the unknown wave parameters (S , Q , U , V for the intensity and polarization state [Kraus, 1966], θ and ϕ for the source colatitude and azimuth in a given reference frame) we search for a solution where the weighted least squared sum of the differences between the wave observations y_i^{obs} (either from Ulysses URAP or from Cassini RPWS) and the model-predicted values y_i^{mod} becomes a minimum:

$$\chi^2 = \sum_{i=1}^N W_i (y_i^{obs} - y_i^{mod}(X_j))^2 = Min \quad (1)$$

The y_i^{obs} represent the squared voltages provided by the instrument measurements (URAP or RPWS). The URAP instrument provides 24 measurements during one Ulysses spin period ($N=24$ in Equation (1)) and the RPWS on Cassini provides 7 simultaneous measurements ($N=7$ in Equation (1)).

The y_i^{mod} represent the theoretical expressions of the measured signals as a function of S , Q , U , V , θ and ϕ as given by Ladreiter et al. [1995] for Cassini RPWS and by Ladreiter et al. [1994] for Ulysses URAP.

The W_i are the weights reflecting the uncertainty of each y_i^{obs} . The W_i are in general proportional to $(y_i^{obs})^{-2}$ defined by the automatic gain control (AGC) value of the observation i to account for the constant relative error in the data. The X_j are the wave parameters to be determined (i.e. $X_j = [S, Q, U, V, \theta, \phi]$) for direction finding. To find the solution for Equation (1) we perform differentiation with respect to X_j :

$$\frac{\partial \chi^2}{\partial X_j} = 0 \quad (2)$$

The value χ^2 is not linear with regard to X_j after differentiation, thus linearisation is required:

$$\frac{\partial \chi^2}{\partial X_j} \bigg|_{\vec{X}^0} = - \frac{\partial^2 \chi^2}{\partial X_j \partial X_k} \bigg|_{\vec{X}^0} \cdot \Delta X_k \quad (3)$$

The term $\partial^2 \chi^2 / (\partial X_j \partial X_k)$ represents a 6 times 6 symmetrical square matrix containing the partial derivatives of χ^2 with respect to X_j and X_k . The matrix element $j = 5$, $k = 6$, for example, denotes $\partial^2 \chi^2 / (\partial \theta \partial \phi)$. Rapid convergence of the iteration process is ensured if Equation 3 denotes a well-posed system of equations. Iteration should be performed until ΔX_k is small. A good initial guess \vec{X}^o (not too far from \vec{X} that minimizes χ^2) is necessary for ensuring rapid convergence of the process.

Equation (3) can be written in the form:

$$b_j = A_{jk} \Delta X_k \quad (4)$$

Since the iteration procedure may be not efficient for ill-posed systems of equations we apply Singular Value Decomposition (SVD) (see e.g. Press et al. [1986]) to see whether or not the matrix A is basically of full rank:

$$\vec{b} = U \Lambda V^T \Delta \vec{X} \quad (5)$$

where the matrices V and U are columnwise composed of the eigenvectors of $A^T A$ and AA^T , respectively. Here $U = V$ since A is symmetrical (T denotes the transpose of a matrix). Λ is a diagonal matrix containing the singular values of A :

$$\Lambda = \begin{pmatrix} \lambda_1 & 0 & \dots & \dots \\ 0 & \lambda_2 & \dots & \dots \\ \vdots & \vdots & \ddots & \dots \\ \vdots & \vdots & \vdots & \lambda_n \end{pmatrix}$$

The singular values λ_i of A correspond to the squareroot of eigenvalues of the matrix AA^T or $A^T A$.

Inverting Equation (5) we finally obtain the system of linearized direction finding equations which was previously solved by iteration (see also Press et al. [1986] and references therein):

$$\Delta \vec{X} = V \Lambda^{-1} U^T \vec{b} \quad (6)$$

where $V \Lambda^{-1} U^T = A^+$ is called the generalized inverse of A and Λ^{-1} is the inverse of Λ containing the inverse of the λ_n :

$$\Lambda^{-1} = \begin{pmatrix} 1/\lambda_1 & 0 & \dots & \dots \\ 0 & 1/\lambda_2 & \dots & \dots \\ \vdots & \vdots & \ddots & \dots \\ \vdots & \vdots & \vdots & 1/\lambda_n \end{pmatrix}$$

Special insight into the equation system can be obtained by inspection of Λ . If the variances of the elements X_j are of similar size, the effective number of linear independent equations can be identified by counting the number of significant singular values, excluding those whose value is 0 or practically 0.

If the number of significant singular values is equal to the number of unknowns in X_j (6 in our case), then the X_j are well-defined by the system of equations. If it is less than the number of unknowns, then the solution vector X_j has no unique solution and the system of equations is ill-conditioned. In constructing our solution vector X_j obtained by iteration using ΔX from Equation (6), we are then free to eliminate the near zero singular values (and the corresponding eigenvectors), reducing the parameter variance to a lower level by simultaneously keeping χ^2 statistically at its minimum value as required by Equation (1). By this technique we avoid a large contribution of poorly defined parameters due to a small noise component on the data, at the expense of a loss of model parameter resolution. Parameter resolution is described by the resolution matrix R (see Connerney [1981] and references therein) relating the solution $X(l)$ using l eigenvectors to the solution X using all eigenvectors (including those associated with small singular values) that represents the traditional least squares solution.

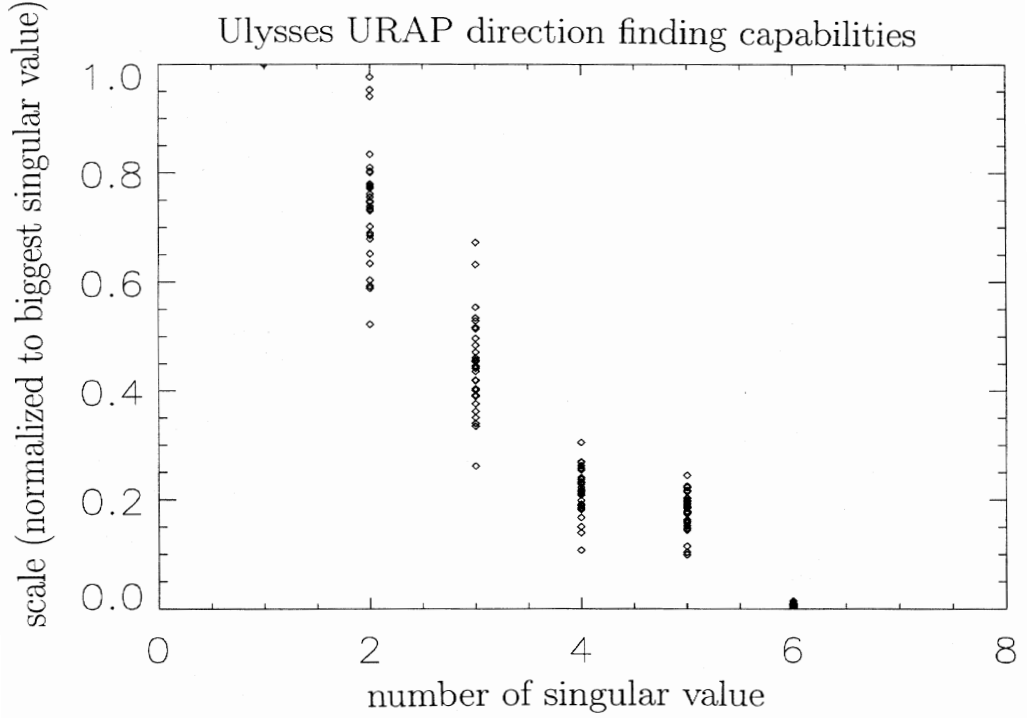


Figure 1: Example of singular values derived from direction finding of Jovian hectometric emission using the Ulysses URAP experiment. Data observed during 40 individual Ulysses spacecraft spins are shown and indicated by diamonds. We notice the small value of the sixth singular value for all rotations investigated.

$$X(l) = R(l)X \quad (7)$$

where $R(l) = V(l)V(l)^T$ and the index l to a matrix denotes the matrix obtained by setting each column i for $i > l$ of the original matrix to zero. If no eigenvector is set to zero then R is the identity matrix; as fewer eigenvectors are admitted in the construction of the solution, the off-diagonal elements of the R matrix grow at the expense of the diagonal elements, denoting a loss of parameter resolution. The off-diagonal elements of the resolution matrix R describe linear combinations of parameters which are zero only if the number of equations in consideration is equal to the number of unknowns.

In Figure 1 we show the singular values λ_1 to λ_6 as derived according to the singular value decomposition analysis for the Ulysses URAP observations of the jovian hectometric emission ($f=540$ kHz) at February 9, 1992, around 0100 spacecraft event time. A HOM storm lasting for more than one hour allowed for continuous observations during some 40 spacecraft spin periods. For each rotation, λ_1 to λ_6 are individually plotted (diamonds) and normalized with respect to λ_1 (set to unity). The overall impression is that λ_6 is considerably smaller than the other singular values indicating that the system of direction finding equations (Equation 4) is not well-posed. The smallest singular value, λ_6 is two orders of magnitude smaller than the largest one, λ_1 . Since the small singular value λ_6 is responsible for high noise propagation from data into parameter space during the

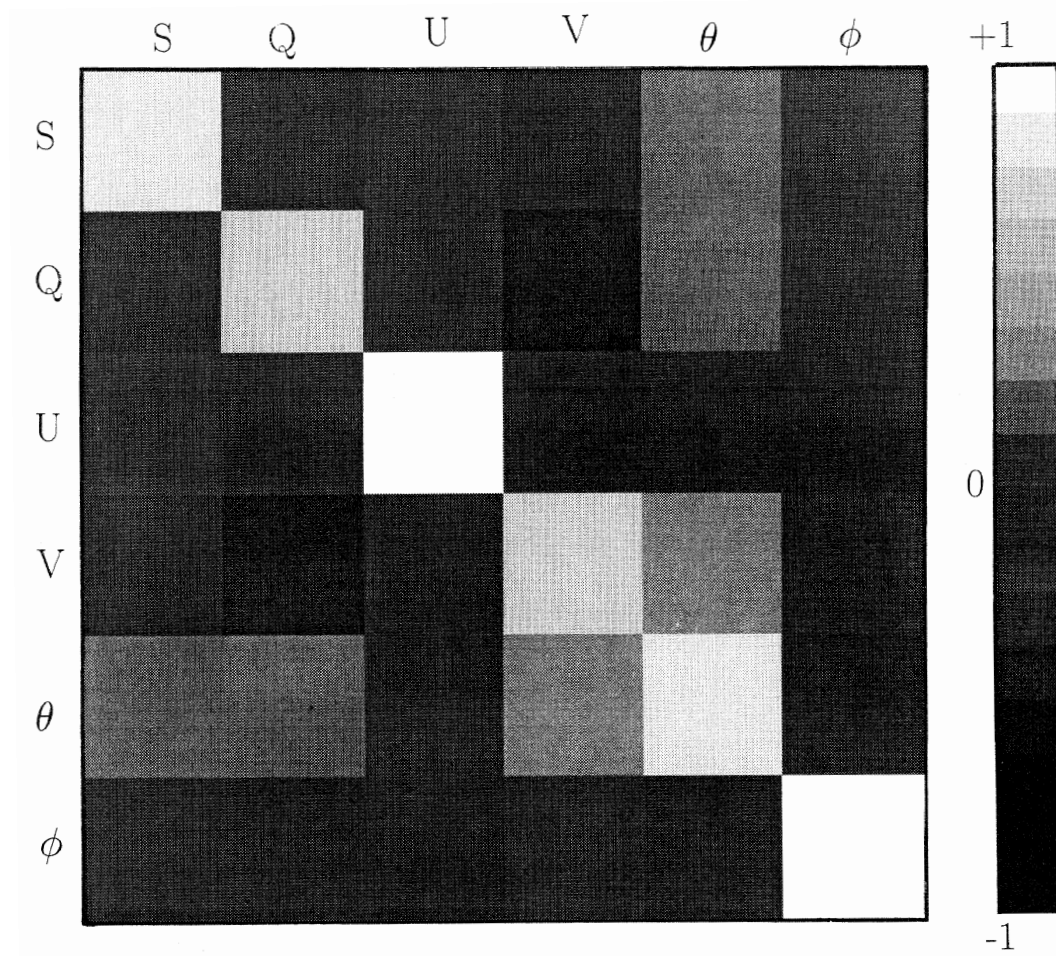


Figure 2: Parameter resolution of the Stokes parameters S , Q , U , V , and the source direction angles θ and ϕ . In case of perfect resolution of all parameters the resolution matrix is identical with the unity matrix. The less a parameter is resolved the more the corresponding diagonal element is deviating from unity. The best resolved parameters are U and ϕ (with corresponding resolution close to unity), the others are less well-defined and show linear dependence which is indicated by non-zero off-diagonal elements (e.g. strong linear dependence between V and θ as indicated by the matrix elements $R_{5,4}$ or $R_{4,5}$ whose values are about $+0.4$, thus considerably different from zero).

inversion (according to Equation (6) its value should be set to zero prior to inversion. The propagation of data noise is then reduced at the expense of loss in parameter resolution as defined by the resolution matrix in Equation (7). An example of parameter resolution for a typical HOM observation during one spacecraft spin is shown in Figure 2. The resolutions of the Stokes parameters S , Q , U , V and the source direction angles θ and ϕ are shown by the diagonal elements of the matrix. Clearly, the parameter U and the source azimuth ϕ are well-defined (resolution very close to unity) whereas the remaining parameters are somewhat poorer resolved showing also some degree of linear dependence. For example the parameters V (degree of circular polarization) and the source colatitude θ are linear dependent, thus they cannot be retrieved independently from each other during the inversion process.

3 Source Size

Some of previous papers [Manning and Fainberg, 1980; Reiner et al., 1993a,b] introduced the source size as unknown parameter in the direction finding analysis of Ulysses URAP data. Since the monopole and dipole antennas of the Ulysses URAP instrument have large antenna patterns, they are hardly sensitive to source widths which are small compared to the characteristic dimensions of the antenna diagram (some 60 deg for a dipole). For illustration we plot in Figure 3 the antenna response of the synthesized dipole (S_{90}) of the Ulysses URAP instrument (crosses) that is modeled for a point source (full line), for a source with 10 deg uniform width (dashed line) and for a source with 20 deg uniform width (dashed dotted line). The data was collected during a period of intense HOM emission around 0100 SCET on February 8, 1992. It can clearly be seen that the antenna responses for the different types of sources (point source, extended sources) is very similar and cannot be discerned by the sparse data (crosses). Since source widths less than some 20 deg cannot be resolved by dipole/monopole antenna systems, the source extension should not be introduced as free parameter when doing direction finding of planetary radio sources which are supposed to have small extensions. In contrast, the source width could be a meaningful parameter when analyzing solar type III radio emissions with generally large source widths.

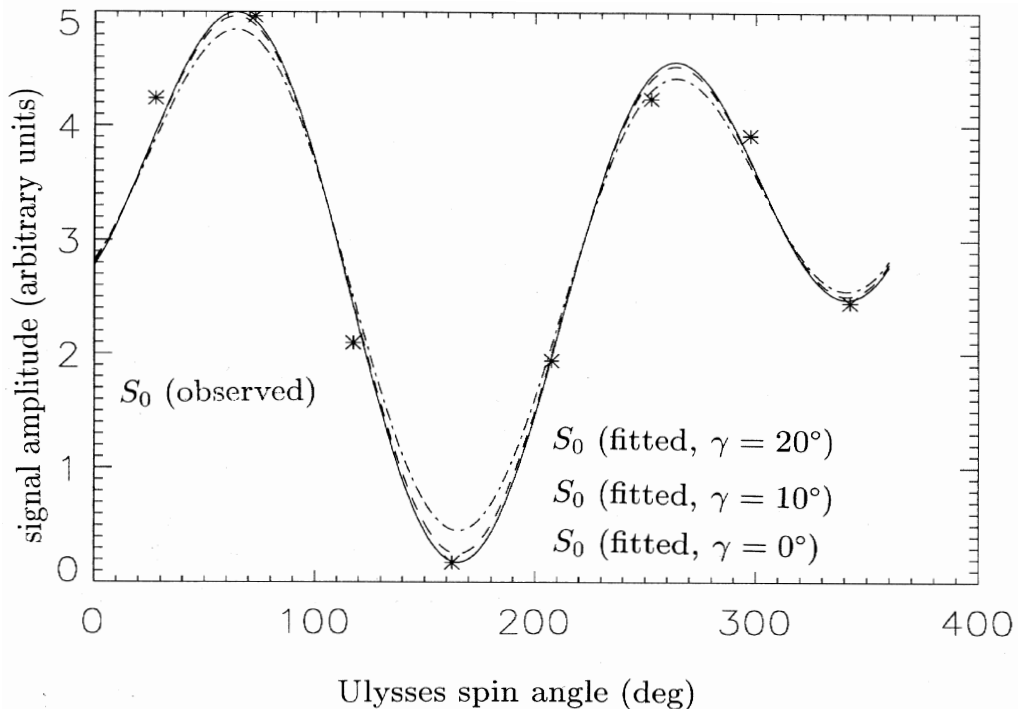


Figure 3: Antenna response of the synthesized dipole (S_{90}) of the Ulysses URAP instrument (crosses) which is modeled for a point source (full line), for a source with 10 deg uniform width (dashed line) and for a source with 20 deg uniform width (dashed dotted line). The data (crosses) was collected during a period of intense HOM emission around 0100 SCET on February 8, 1992. Notice that the instrument cannot discern point sources from small sources.

4 Selected Results

The most spectacular results associated with direction finding of planetary non-thermal radio emissions have been provided by the Ulysses URAP experiment monitoring the Jovian and solar radio emissions. Concerning the Jovian emissions, investigations were performed by Reiner et al. [1993a,b] analyzing the Jovian hectometric and narrowband kilometric emission, and Ladreiter et al. [1994] who investigated the Jovian hectometric and broadband kilometric emissions. The results in terms of source position on the Jovian hectometric components as derived by Reiner et al. [1993a] and Ladreiter et al. [1994] are significantly different which we suppose is due to *a)* different assumptions on the antenna calibration and *b)* somewhat different types of methods used. The sources of Reiner et al. [1993] are located at relatively low magnetic latitudes, $L=4$ to 6 (L =dipole shell parameter) whereas the sources of Ladreiter et al. [1994] are positioned at $L=8$ to 10 . Figure 4 shows an example of HOM source locations as found by Ladreiter et al. [1994].

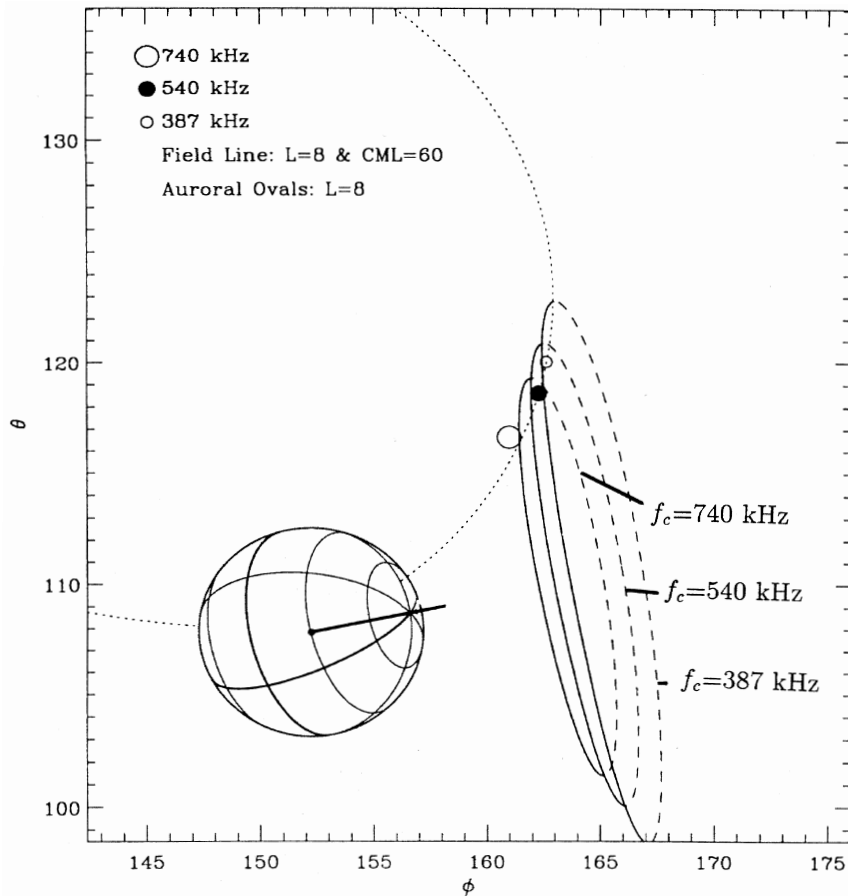


Figure 4: Average source position for the HOM event occurring on February 8, 1992 0140 to 0225 Ulysses event time at $f = 387, 540$ and 740 kHz. We plotted for reference the auroral ovals at $L=8$ at the three frequencies and the corresponding field line at $CML=60$ deg. The sources of the different frequencies are nicely aligned at this field line when assuming that the wave frequency at the source equals the local electron gyrofrequency (from Ladreiter et al. [1994]).

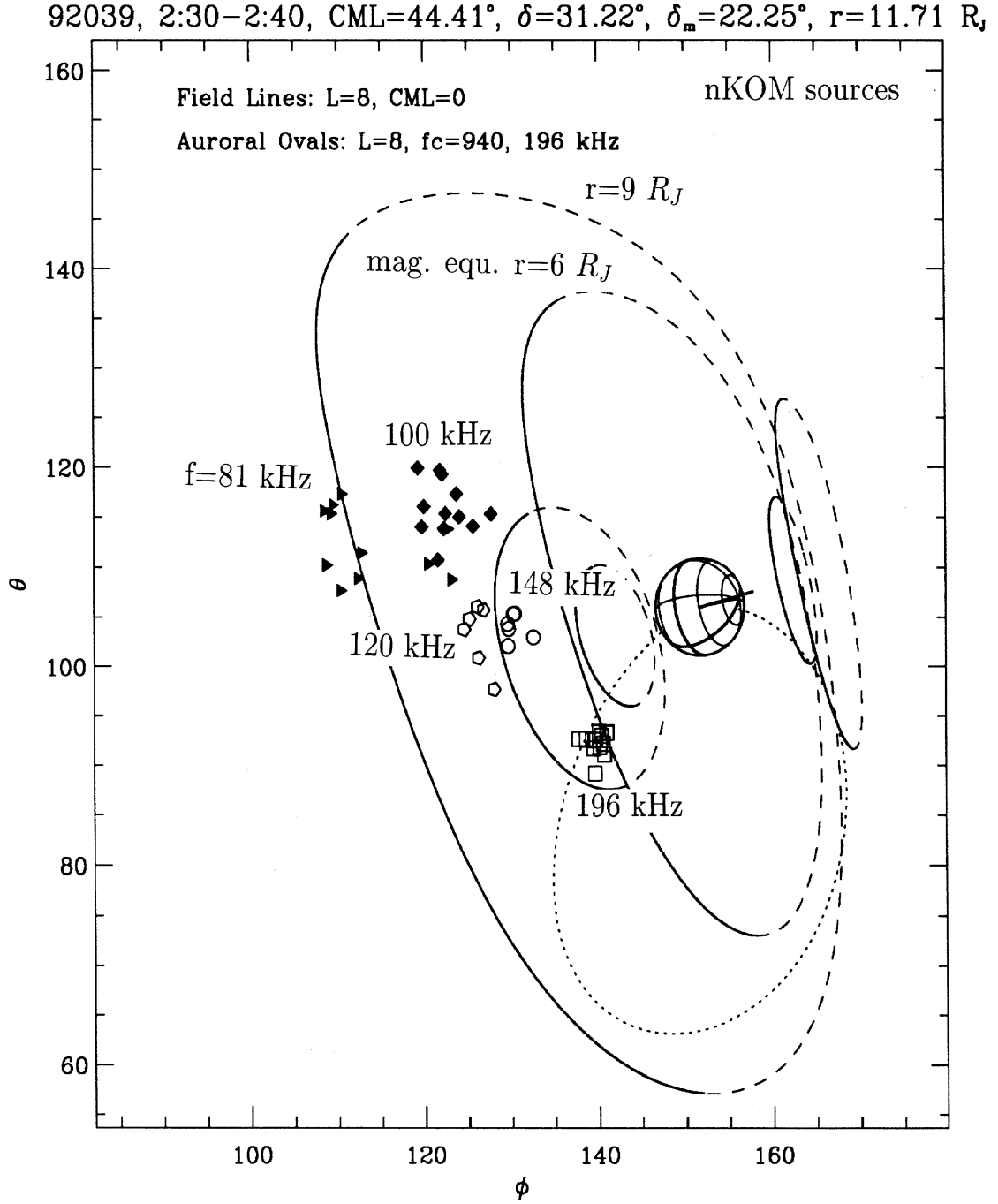


Figure 5: Source location of the narrowband kilometric emission as observed at February 9, 1992, from 0230 to 0240 SCET. Direction finding results at $f=196$ kHz (rectangles), $f=148$ kHz (circles), $f=120$ kHz (polygons), $f=100$ kHz (full diamonds), and $f=81$ kHz (full triangles) are shown. For reference, we plotted the magnetic dipole equator at $r=6$ and 9 Jovian radii R_J from the Jovian center, respectively. There is a systematic drift in source location, depending on frequency. The highest frequency ($f=196$ kHz) source is located some $6 R_J$ from Jupiter near the magnetic equator whereas the lowest frequency source ($f=82$ kHz) is $9 R_J$ from Jupiter.

The HOM is located at high latitudes, distinct from the Io flux tube. Straight line propagation of the radiation is assumed and the sources are supposed to be located at the 3D intersection of the line of sight with the respective electron gyrofrequency contour. As seen in Figure 4, consistent source location (in terms of L shell) is found for 3 frequencies at $L \approx 8$. Figure 5 shows source location of the jovian narrowband kilometric emission which is located near the magnetic equator at 6 to 9 R_J from Jupiter depending on frequency. Assuming that the sources are located at regions where the wave frequency equals the local plasma frequency, the present direction finding results can be used as diagnostic tool for the plasma density pattern in the Io torus.

5 Conclusion

When summarizing the principal aspects of the present investigation we can emphasize some main characteristics for direction finding analyses.

1. Direction finding is a powerful method for retrieval of information on planetary but also solar radio emissions.
2. For accurate direction finding, the properties of the antenna/receiver system have to be known as accurate as possible.
3. The source diameter of planetary radio sources should not be included as variable during the inversion procedure. Apparent source sizes tend to be extremely large (due to insufficient spatial resolution of the monopole/dipole antennas) and seem to influence other derived wave parameters systematically.
4. Analyses using generalized inversion techniques help to obtain detailed information on the stability/accuracy of the solution.